

Numerical Solution of a Class of Singularly Perturbed Parabolic Reaction-Diffusion Problem

Chenhui Zhao, Yulan Wang

Inner Mongolia University of Technology, Hohhot Inner Mongolia

Email: 18435122110@163.com

Received: Jun. 11th, 2019; accepted: Jun. 21st, 2019; published: Jun. 28th, 2019

Abstract

The singularly perturbed problem's high accuracy numerical method is always needed. In this paper, barycentric Lagrange interpolation collocation method (BLICM) is proposed for solving a class of singularly perturbed parabolic reaction-diffusion problem. Compared with other methods, the numerical experiment shows BLICM is a high precision method to solve this class of problems.

Keywords

Singular Perturbation, Barycentric Lagrange Interpolation Collocation Method, Parabolic Reaction-Diffusion Problem

一类奇异摄动抛物型反应扩散问题的数值解

赵辰辉, 王玉兰

内蒙古工业大学, 内蒙古 呼和浩特

Email: 18435122110@163.com

收稿日期: 2019年6月11日; 录用日期: 2019年6月21日; 发布日期: 2019年6月28日

摘要

奇异摄动问题一直需要高精度的数值方法, 本文提出了重心拉格朗日插值配点法来求解一类奇异摄动抛物型反应扩散问题, 与其他方法相比, 数值实验表明该方法是解决这类问题的一种高精度方法。

文章引用: 赵辰辉, 王玉兰. 一类奇异摄动抛物型反应扩散问题的数值解[J]. 应用数学进展, 2019, 8(6): 1181-1191.
DOI: 10.12677/aam.2019.86136

关键词

奇异摄动, 重心拉格朗日插值配点法, 抛物型反应扩散问题

Copyright © 2019 by author(s) and Hans Publishers Inc.

This work is licensed under the Creative Commons Attribution International License (CC BY).

<http://creativecommons.org/licenses/by/4.0/>



Open Access

1. 引言

我们考虑下列的奇异摄动抛物型反应扩散问题:

$$\begin{cases} \frac{\partial u}{\partial t} - \varepsilon_1 \frac{\partial^2 u}{\partial x^2} + \alpha_1 u + \alpha_2 v + \alpha_3 r = f_1(x, t), \\ \frac{\partial v}{\partial t} - \varepsilon_2 \frac{\partial^2 v}{\partial x^2} + \beta_1 u + \beta_2 v + \beta_3 r = f_2(x, t), (x, t) \in [0, 1] \times [0, 1], \\ \frac{\partial r}{\partial t} - \varepsilon_3 \frac{\partial^2 r}{\partial x^2} + \gamma_1 u + \gamma_2 v + \gamma_3 r = f_3(x, t), \end{cases} \quad (1)$$

具有初始边界条件

$$\begin{aligned} u(x, 0) &= f_0(x), v(x, 0) = g_0(x), r(x, 0) = s_0(x), x \in [0, 1] \\ u(0, t) &= f_1(t), u(1, t) = f_2(t), \\ v(0, t) &= g_1(t), v(1, t) = g_2(t), t \in [0, 1] \\ r(0, t) &= s_1(t), r(1, t) = s_2(t), \end{aligned} \quad (2)$$

其中 ε 是任意小参数, $\alpha_i, \beta_i, \gamma_i$ 为给定常数, $f_1(x, t), f_2(x, t), f_3(x, t), f_1(t), f_2(t), g_1(t), g_2(t), s_1(t), s_2(t)$ 是已知函数, $u(x, t), v(x, t), r(x, t)$ 分别是未知函数。

奇异摄动抛物型反应扩散问题[1] [2] [3] [4] [5]在热科学和力学中有广泛的应用, 有一些有价值的努力专注于找到解决问题的分析和数值方法[6]-[11]。在[12] [13] [14] [15] [16]中, J.P. Berrut引入了重心拉格朗日插值, 并研究了它的数值稳定性和收敛性。重心拉格朗日插值在切比雪夫节点处无条件稳定。在[17] [18]中, Li和Wang给出了BLICM的算法和程序, 用于普通的微分方程, 积分方程和差分积分方程以及偏微分方程等。在[19]-[24]中, Wang运用了BLICM解决耦合粘性Burgers方程, 奇异扰动问题和混沌系统。在[25]中, BLICM被提出用于求解第二类线性和非线性高维Fredholm积分方程。参考文献[17]-[26]的结果表明BLICM具有高精度, 良好的稳定性和收敛性。在本文中, BLICM被提出用于求解一类奇异摄动抛物型反应扩散问题。

2. BLICM 的描述

我们考虑规则区域 $\Omega = [0, 1] \times [0, 1]$, 区间 $[0, 1]$ 被分成 M 个不同的节点, 区间 $[0, 1]$ 也被分成 N 个不同的节点。

为了提高计算精度, 我们选则 Chebyshev 节点, 切比雪夫节点计算公式如下:

$$\begin{aligned}x_i &= -\cos\left(\frac{i-1}{M-1}\right)\pi, i=1,2,\dots,M, \\t_j &= -\cos\left(\frac{j-1}{N-1}\right)\pi, j=1,2,\dots,N.\end{aligned}\quad (3)$$

节点 (x_i, t_j) 处的 $u(x, t), v(x, t)$ 和 $r(x, t)$ 的重心插值可写为:

$$\begin{aligned}u(x, t) &= \sum_{i=1}^M \sum_{j=1}^N \xi_i(x) \eta_j(t) u(x_i, t_j), \\v(x, t) &= \sum_{i=1}^M \sum_{j=1}^N \xi_i(x) \eta_j(t) v(x_i, t_j), \\r(x, t) &= \sum_{i=1}^M \sum_{j=1}^N \xi_i(x) \eta_j(t) r(x_i, t_j),\end{aligned}\quad (4)$$

$$\text{其中, } \xi_i(x) = \frac{\prod_{k=1, k \neq i}^M (x - x_k)}{\prod_{k=1, k \neq i}^M (x_i - x_k)}, i=1,2,\dots,M, \quad \eta_j(t) = \frac{\prod_{k=1, k \neq j}^N (t - t_k)}{\prod_{k=1, k \neq j}^N (t_j - t_k)}, j=1,2,\dots,N.$$

使用公式(4), 节点上函数 $u(x, t)$ 的 $l+k$ 阶偏导数可表示为:

$$\begin{aligned}\frac{\partial^{l+k} u}{\partial x^l \partial t^k} &= \sum_{i=1}^M \sum_{j=1}^N \xi_i^{(l)}(x) \eta_j^{(k)}(t) u(x_i, t_j), l, k = 1, 2, \dots, \\&\frac{\partial^{l+k} v}{\partial x^l \partial t^k} = \sum_{i=1}^M \sum_{j=1}^N \xi_i^{(l)}(x) \eta_j^{(k)}(t) v(x_i, t_j), l, k = 1, 2, \dots, \\&\frac{\partial^{l+k} r}{\partial x^l \partial t^k} = \sum_{i=1}^M \sum_{j=1}^N \xi_i^{(l)}(x) \eta_j^{(k)}(t) r(x_i, t_j), l, k = 1, 2, \dots,\end{aligned}\quad (5)$$

在节点 (x_p, t_q) 处, 偏导数的函数值定义为:

$$\begin{aligned}u^{(l,k)}(x_p, t_q) &= \frac{\partial^{l+k} u}{\partial x^l \partial t^k}(x_p, t_q) = \sum_{i=1}^M \sum_{j=1}^N \xi_i^{(l)}(x_p) \eta_j^{(k)}(t_q) u(x_i, t_j), p=1,2,\dots,M; q=1,2,\dots,N, \\v^{(l,k)}(x_p, t_q) &= \frac{\partial^{l+k} v}{\partial x^l \partial t^k}(x_p, t_q) = \sum_{i=1}^M \sum_{j=1}^N \xi_i^{(l)}(x_p) \eta_j^{(k)}(t_q) v(x_i, t_j), p=1,2,\dots,M; q=1,2,\dots,N, \\r^{(l,k)}(x_p, t_q) &= \frac{\partial^{l+k} r}{\partial x^l \partial t^k}(x_p, t_q) = \sum_{i=1}^M \sum_{j=1}^N \xi_i^{(l)}(x_p) \eta_j^{(k)}(t_q) r(x_i, t_j), p=1,2,\dots,M; q=1,2,\dots,N.\end{aligned}\quad (6)$$

令 $x^0 = [x_1, x_2, \dots, x_M]^T$, $t^0 = [t_1, t_2, \dots, t_N]^T$ 分别定义为 x 轴和 t 轴, 由张量型节点坐标组成的矩阵 X 和 T 分别定义为:

$$X = \left[\left(x^0 \right)^T, \left(x^0 \right)^T, \dots, \left(x^0 \right)^T \right]^T, T = \left[t^0, t^0, \dots, t^0 \right]. \quad (7)$$

x, t 是由矩阵 X, T 拉伸的 $(N \times M)$ 维列向量:

$$x = [X_1, X_2, \dots, X_{M \times N}]^T, t = [T_1, T_2, \dots, T_{M \times N}]^T. \quad (8)$$

向量 x, t 和向量 x^0, t^0 的分量之间的关系如下:

$$X_k = X_{(i-1)N+j} = x_i, T_k = T_{(i-1)N+j} = t_j, i=1,2,\dots,M; J=1,2,\dots,N; k=1,2,\dots,M \times N. \quad (9)$$

假设 u 和 $u^{(l,k)}$ 是由 $u(x_i, t_j)$ 和 $u^{(l,k)}(x_i, t_j)$ $(i=1, 2, \dots, M; j=1, 2, \dots, N)$ 组成的列向量，即：

$$u = [u_1, u_2, \dots, u_{M \times N}]^T, \quad u^{(l,k)} = [u_1^{(l,k)}, u_2^{(l,k)}, \dots, u_{M \times N}^{(l,k)}]^T,$$

$$u_p = u(X_p, T_p), \quad u_p^{(l,k)} = u^{(l,k)}(X_p, T_p), \quad p = 1, 2, \dots, M \times N.$$

$$v = [v_1, v_2, \dots, v_{M \times N}]^T, \quad v^{(l,k)} = [v_1^{(l,k)}, v_2^{(l,k)}, \dots, v_{M \times N}^{(l,k)}]^T,$$

$$v_p = v(X_p, T_p), \quad v_p^{(l,k)} = v^{(l,k)}(X_p, T_p), \quad p = 1, 2, \dots, M \times N.$$

$$r = [r_1, r_2, \dots, r_{M \times N}]^T, \quad r_p^{(l,k)} = [r_1^{(l,k)}, r_2^{(l,k)}, \dots, r_{M \times N}^{(l,k)}]^T,$$

$$r_p = r(X_p, T_p), \quad r_p^{(l,k)} = r^{(l,k)}(X_p, T_p), \quad p = 1, 2, \dots, M \times N.$$

因此，(4)可写成下列的矩阵形式：

$$u^{(l,k)} = D^{(l,k)}u, \quad v^{(l,k)} = D^{(l,k)}v, \quad r^{(l,k)} = D^{(l,k)}r. \quad (10)$$

在上面的公式中， $D^{(l,k)} = C^{(l)} \otimes D^{(k)}$ 是矩阵 $C^{(l)}$ 和 $D^{(k)}$ 的Kronecker乘积，也被称为在节点 $\{(x_i, t_j), i=1, 2, \dots, M; j=1, 2, \dots, N\}$ 的 (l, k) 阶部分差分矩阵。 $C^{(l)}$ 是 x 方向节点上的 l 阶差分矩阵， $D^{(k)}$ 是 t 方向节点上的 k 阶差分矩阵。因此，(1)可写成以下矩阵形式：

$$\begin{bmatrix} D^{(0,1)} - \varepsilon_1 D^{(2,0)} + \alpha_1 I & \alpha_2 I & \alpha_3 I \\ \beta_1 I & D^{(0,1)} - \varepsilon_2 D^{(2,0)} + \beta_2 I & \beta_3 I \\ \gamma_1 I & \gamma_2 I & D^{(0,1)} - \varepsilon_3 D^{(2,0)} + \gamma_3 I \end{bmatrix} \begin{bmatrix} u \\ v \\ r \end{bmatrix} = \begin{bmatrix} f_1 \\ f_2 \\ f_3 \end{bmatrix} \quad (11)$$

将公式(3)代入初始边界条件(2)，我们可以得到关于 $u(x, t), v(x, t), r(x, t)$ 在 $q=1, 2, \dots, N$ 的初始边界条件的离散方程：

$$\begin{aligned} \sum_{i=1}^M \sum_{j=1}^N \xi_i(x_p) \eta_j(0) u_{ij} &= f_0(x_p), & \sum_{i=1}^M \sum_{j=1}^N \xi_i(0) \eta_j(t_q) u_{ij} &= f_1(t_q), & \sum_{i=1}^M \sum_{j=1}^N \xi_i(1) \eta_j(t_q) u_{ij} &= f_2(t_q), \\ \sum_{i=1}^M \sum_{j=1}^N \xi'_i(x_p) \eta'_j(0) v_{ij} &= g_0(x_p), & \sum_{i=1}^M \sum_{j=1}^N \xi'_i(0) \eta'_j(t_q) v_{ij} &= g_1(t_q), & \sum_{i=1}^M \sum_{j=1}^N \xi'_i(1) \eta'_j(t_q) v_{ij} &= g_2(t_q), \\ \sum_{i=1}^M \sum_{j=1}^N \xi''_i(x_p) \eta''_j(0) r_{ij} &= s_0(x_p), & \sum_{i=1}^M \sum_{j=1}^N \xi''_i(0) \eta''_j(t_q) r_{ij} &= s_1(t_q), & \sum_{i=1}^M \sum_{j=1}^N \xi''_i(1) \eta''_j(t_q) r_{ij} &= s_2(t_q), \end{aligned} \quad (12)$$

在本文中，我们用置换法来施加初始边界条件。

3. 数值算例

在此部分中，我们展示了用此数值方法得到的数值结果，从而求出下面例子的近似解。

例 1 我们考虑以下具有不连续源项的奇异摄动抛物型反应扩散问题[8]：

$$\begin{cases} \frac{\partial u}{\partial t} - \varepsilon_1 \frac{\partial^2 u}{\partial x^2} + 5u - tv = f_1(x, t), \\ \frac{\partial v}{\partial t} - \varepsilon_2 \frac{\partial^2 v}{\partial x^2} - tu + 5(1+xt)v - r = f_2(x, t), \\ \frac{\partial r}{\partial t} - \varepsilon_3 \frac{\partial^2 r}{\partial x^2} - 2u - (1+x^2)v + (7+xt)r = f_3(x, t), \end{cases} \quad (13)$$

具有初始边界条件:

$$u(0,t) = v(0,t) = r(0,t) = 0, u(1,t) = v(1,t) = r(1,t) = 0, u(x,0) = v(x,0) = r(x,0) = 0, \quad (14)$$

其中

$$\begin{aligned} f_1(x,t) &= \begin{cases} 2+x+t, & 0 \leq x \leq 0.5, \\ 1, & 0.5 < x \leq 1, \end{cases} \\ f_2(x,t) &= \begin{cases} 2 & 0 \leq x \leq 0.5, \\ t, & 0.5 < x \leq 1, \end{cases} \end{aligned} \quad (15)$$

和

$$f_3(x,t) = \begin{cases} 1+x, & 0 \leq x \leq 0.5, \\ x^2 + t, & 0.5 < x \leq 1. \end{cases}$$

图1和图2分别给出了选取不同的节点 M 和 N 时得到的数值解。表1给出了参数 N 变为2倍时的数值结果, 在表2中, 得到了参数 N 除以2, 参数 Δt 除以2时的数值结果。在这种情况下, 观察到一阶均匀收敛。 ε 的值越大, 结果越小, 当 ε 的值达到某一值时, 数值结果是稳定的。从表1和表2我们可以看出, 此方法比以前的方法具有更高的精度, 我们推断, 时间离散化的误差控制了数值格式的全局误差。

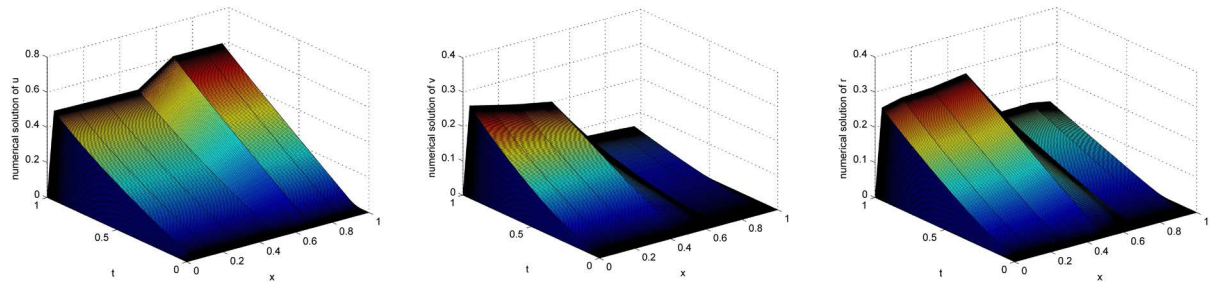


Figure 1. Surface plot of the Example 1 for $\varepsilon_1 = 10^{-9}, \varepsilon_2 = 10^{-5}, \varepsilon_3 = 10^{-3}$ and $N = 256, M = 8$

图1. 例1的数值解图当 $\varepsilon_1 = 10^{-9}, \varepsilon_2 = 10^{-5}, \varepsilon_3 = 10^{-3}$ 和 $N = 256, M = 8$

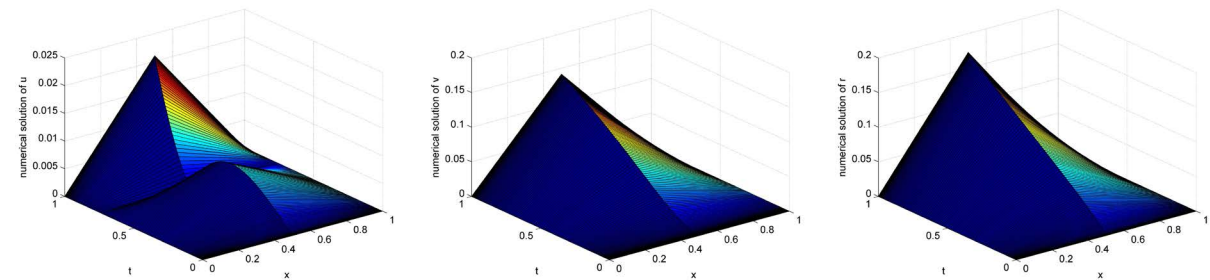


Figure 2. Surface plot of the Example 1 for $\varepsilon_1 = 10^{-9}, \varepsilon_2 = 10^{-5}, \varepsilon_3 = 10^{-3}$ and $N = 128, M = 2$

图2. 例1的数值解图当 $\varepsilon_1 = 10^{-9}, \varepsilon_2 = 10^{-5}, \varepsilon_3 = 10^{-3}$ 和 $N = 128, M = 2$

Table 1. Comparison of maximum point-wise errors and $\varepsilon_1, \varepsilon_2, \varepsilon_3$ uniform rate of convergence for the example 1

表1. 例1最大点积误差与 $\varepsilon_1, \varepsilon_2, \varepsilon_3$ 均匀收敛速度的比较

	Ref. [8] Present method								
$\varepsilon_1 = 10^{-j}$	$N = 128$ $M = 2$	$N = 256$ $M = 8$	$N = 512$ $M = 32$	$N = 1024$ $M = 128$	$N = 128$ $M = 2$	$N = 256$ $M = 8$	$N = 512$ $M = 32$	$N = 1024$ $M = 128$	
$j = 1$	3.22E-02	1.71E-02	5.92E-03	1.63E-03	2.33E-04	1.27E-06	4.27E-08	3.73E-10	

Continued

$j = 2$	3.84E-02	1.84E-02	5.88E-03	1.59E-03	2.45E-04	1.34E-06	4.34E-08	3.91E-10
$j = 3$	4.00E-02	1.90E-02	6.05E-03	1.63E-03	3.05E-04	2.08E-06	5.02E-08	4.21E-10
$j = 4$	4.24E-02	1.98E-02	6.31E-03	1.70E-03	3.78E-04	2.57E-06	5.17E-08	4.59E-10
$j = 5$	4.42E-02	2.24E-02	8.90E-03	2.84E-03	4.02E-04	2.96E-06	5.63E-08	5.10E-10
$j = 8$	4.42E-02	2.24E-02	8.90E-03	2.84E-03	4.28E-04	3.03E-06	6.12E-08	5.33E-10
$j = 10$	4.42E-02	2.24E-02	8.90E-03	2.84E-03	4.28E-04	3.03E-06	6.12E-08	5.33E-10
$j = 12$	4.42E-02	2.42E-02	8.90E-03	2.84E-03	4.28E-04	3.03E-06	6.12E-08	5.33E-10

Table 2. Comparison of maximum point-wise errors and $\varepsilon_1, \varepsilon_2, \varepsilon_3$ uniform rate of convergence for the Example 1**表2.** 例1最大点积误差与 $\varepsilon_1, \varepsilon_2, \varepsilon_3$ 均匀收敛速度的比较

Ref. [8] Present method								
$\varepsilon_1 = 10^{-j}$	$N = 128$ $M = 2$	$N = 256$ $M = 8$	$N = 512$ $M = 32$	$N = 1024$ $M = 128$	$N = 128$ $M = 2$	$N = 256$ $M = 8$	$N = 512$ $M = 32$	$N = 1024$ $M = 128$
$j = 1$	3.22E-02	2.68E-02	1.71E-02	1.06E-02	2.33E-04	2.02E-05	4.01E-07	3.21E-09
$j = 2$	3.84E-02	2.89E-02	1.84E-02	1.07E-02	2.45E-04	2.31E-05	4.21E-07	3.33E-09
$j = 3$	4.00E-02	2.98E-02	1.90E-02	1.09E-02	3.05E-04	2.76E-05	4.83E-07	3.89E-09
$j = 4$	4.24E-02	3.05E-02	1.93E-02	1.11E-02	3.78E-04	3.03E-05	5.21E-07	4.15E-09
$j = 5$	4.42E-02	3.25E-02	2.01E-02	1.14E-02	4.02E-04	3.28E-05	5.38E-07	4.27E-09
$j = 8$	4.42E-02	3.25E-02	2.01E-02	1.15E-02	4.28E-04	3.56E-05	5.92E-07	4.83E-09
$j = 10$	4.42E-02	3.25E-02	2.01E-02	1.15E-02	4.28E-04	3.56E-05	5.92E-07	4.83E-09
$j = 12$	4.42E-02	3.25E-02	2.01E-02	1.15E-02	4.28E-04	3.56E-05	5.92E-07	4.83E-09

表3例举了当 ε , N 和 t 选取不同的值时, 实例1的算法所需的迭代次数。可以观察到, 当 ε 较大时, 迭代次数随着 N 略微减小; 但对于取值小的 ε , 只需要一次迭代。

Table 3. Number of iterations required by the algorithm for Example 1**表3.** 例1算法所需的迭代次数

Ref. [8] Present method					
$\varepsilon_1 = 10^{-j}$	$N = 128$ $M = 2$	$N = 256$ $M = 8$	$N = 512$ $M = 32$	$N = 1024$ $M = 128$	$N = 2048$ $M = 512$
$j = 1$	5	4	3	3	2
$j = 2$	2	2	2	1	1
$j = 3$	1	1	1	1	1
$j = 4$	1	1	1	1	1
$j = 5$	1	1	1	1	1
$j = 6$	1	1	1	1	1
$j = 7$	1	1	1	1	1
$j = 8$	1	1	1	1	1

例 2: 我们考虑以下的时间延迟奇异摄动反应扩散问题[9]:

$$\begin{cases} \frac{\partial u}{\partial t} - \varepsilon_1 \frac{\partial^2 u}{\partial x^2} + 2.1u - (1-x)v - (1+x)r = 16x^2(1-x)^2, \\ \frac{\partial v}{\partial t} - \varepsilon_2 \frac{\partial^2 v}{\partial x^2} - xu + (1.1+x)v - xr = t^2, \\ \frac{\partial r}{\partial t} - \varepsilon_3 \frac{\partial^2 r}{\partial x^2} - (2+x)u - (1-x)v - (3.1+x)r = -16x^2(1-x)^2, \end{cases} \quad (16)$$

具有初始边界条件

$$u(0,t) = v(0,t) = r(0,t) = 0, \quad u(1,t) = v(1,t) = r(1,t) = 0.$$

我们计算了对不同 ε 值的最大误差, 图3和表4展现了相应结果。与Shishkin的方法相比, 通过本方法获得的最大误差更小。这表明此方法具有更高的精确度, 可以看到, 随着 ε 值的增加, 误差变小。

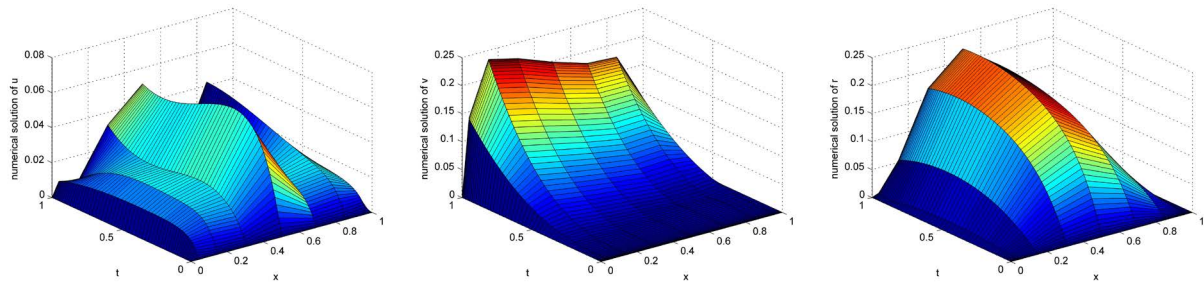


Figure 3. Numerical solution of Example 2 for $\varepsilon_1 = 10^{-1}$, $\varepsilon_2 = 10^{-2}$, $\varepsilon_3 = 10^{-3}$ and $N = 64, M = 8$

图3. 对 $\varepsilon_1 = 10^{-1}$, $\varepsilon_2 = 10^{-2}$, $\varepsilon_3 = 10^{-3}$ 和 $N = 64, M = 8$ 时例 2 的数值解

Table 4. Comparison of maximum point-wise errors and convergence rate for the Example 2

表4. 比较例2的最大点误差和收敛速度

Ref. [9] Present method								
$\varepsilon_1 = 10^{-j}$	$N = 32$	$N = 64$	$N = 128$	$N = 256$	$N = 32$	$N = 64$	$N = 128$	$N = 256$
	$t = 0.1$	$t = 0.1/4$	$t = 0.1/4^2$	$t = 0.1/4^3$	$t = 0.1$	$t = 0.1/4$	$t = 0.1/4^2$	$t = 0.1/4^3$
$j = 0$	8.01E-02	2.90E-02	9.95E-03	2.75E-03	3.03E-03	1.08E-03	3.27E-04	2.08E-06
$j = 1$	1.70E-01	6.88E-02	1.99E-02	5.19E-03	3.17E-03	1.27E-03	3.62E-04	2.16E-06
$j = 2$	2.44E-01	9.34E-02	2.65E-02	6.86E-03	3.58E-03	2.45E-03	3.76E-04	2.53E-06
$j = 3$	2.57E-01	9.77E-02	2.77E-02	7.16E-03	4.02E-03	2.87E-03	4.05E-04	3.21E-06
$j = 4$	2.59E-01	9.81E-02	2.78E-02	7.17E-03	4.55E-03	2.99E-03	4.16E-04	3.45E-06
$j = 5$	2.59E-01	9.81E-02	2.78E-02	7.17E-03	4.55E-03	2.99E-03	4.16E-04	3.45E-06
$j = 6$	2.59E-01	9.81E-02	2.78E-02	7.17E-03	4.55E-03	2.99E-03	4.16E-04	3.45E-06

例 3:

$$\begin{cases} \frac{\partial u}{\partial t} - \varepsilon_1 \frac{\partial^2 u}{\partial x^2} + (5+xt)u - (x^2+t^2)v - (2+xt)r = 2(1-e^{-t}) + 5t \cos(xt), \\ \frac{\partial v}{\partial t} - \varepsilon_2 \frac{\partial^2 v}{\partial x^2} - 5xte^{-x}u + (6+\cos(xt))v - \cos(xt)r = (10x+1)t(x^2+t^2 - 5 \sin(xt)), \\ \frac{\partial r}{\partial t} - \varepsilon_3 \frac{\partial^2 r}{\partial x^2} - 3xe^{-t}u - (xt+\sin(x+t))v + (5+(x+1)e^{-xt})r = -3t \cos(x+t). \\ u(0,t) = u(1,t) = 0, t \in [0,1], u(x,0) = 0, x \in [0,1]. \end{cases} \quad (17)$$

我们选取参数 $\varepsilon_1 = 10^{-8}, \varepsilon_2 = 10^{-6}, \varepsilon_3 = 10^{-4}$ 和 $N = 60, M = 64$, 初始条件 $u(x, 0) = v(x, 0) = r(x, 0) = 0$, 边界条件 $u(0, y) = v(0, y) = r(0, y) = 0$ 。图4显示了方程组的数值近似值, 为了将我们的算法与另一种经典的方法比较, 表5显示了与之前相同的 $\varepsilon_1, \varepsilon_2, \varepsilon_3$ 值的最大误差。从中可以看出, 在这种情况下, 最大误差的大小与表中相似, 但小于表中所示的误差。根据所考虑的问题, 使用重心插值配点法得到的误差有时会更好, 有时会更差点。

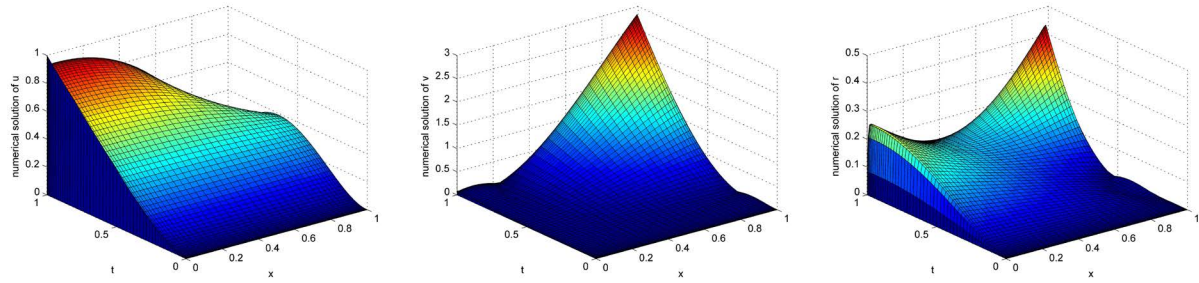


Figure 4. The numerical solution for Example 3 at $\varepsilon_1 = 10^{-8}, \varepsilon_2 = 10^{-6}, \varepsilon_3 = 10^{-4}$

图 4. 当 $\varepsilon_1 = 10^{-8}, \varepsilon_2 = 10^{-6}, \varepsilon_3 = 10^{-4}$ 时例 3 的数值解

Table 5. Comparison of maximum errors and orders of convergence of Example 3
表5. 比较例3的最大误差和收敛阶数

Present method			Ref. [5]					
ε_3	$N = 366$ $M = 16$	$N = 144$ $M = 64$	$N = 288$ $M = 128$	$N = 5766$ $M = 256$	$N = 366$ $M = 16$	$N = 144$ $M = 64$	$N = 288$ $M = 128$	$N = 5766$ $M = 256$
2^{-5}	0.574E-1	0.332E-1	0.160E-1	0.406E-2	0.895E-1	0.392E-1	0.188E-1	0.567E-2
	0.184	1.071	1.352	1.456	0.571	1.060	1.728	1.731
2^{-7}	0.573E-1	0.221E-1	0.088E-1	0.466E-2	0.901E-1	0.392E-1	0.188E-1	0.568E-2
	0.188	0.998	1.453	1.624	0.528	1.060	1.726	1.729
2^{-9}	0.874E-1	0.208E-1	0.074E-1	0.367E-2	0.947E-1	0.390E-1	0.187E-1	0.567E-2
	0.435	0.932	1.533	1.756	0.595	1.062	1.722	1.726
2^{-11}	0.084E-1	0.321E-1	0.096E-1	0.427E-2	0.109E-1	0.423E-1	0.186E-1	0.563E-2
	0.430	1.045	1.629	1.834	0.530	1.186	1.723	1.727
$d_i^{N,M}$	0.403E-1	0.314E-1	0.091E-1	0.513E-2	0.109E+0	0.425E-1	0.188E-1	0.691E-2
P_i^{uni}	0.228	1.048	1.032	1.425	0.529	1.175	1.444	1.525

为了比较两种算法的计算成本, 我们在表6中显示了几个N和M值所需的CPU时间, 选择固定值 $(\varepsilon_1 = 10^{-8}, \varepsilon_2 = 10^{-6}, \varepsilon_3 = 10^{-4})$ 作为扩散参数。相对于与经典的方法比较, 当n值增加时, 我们的方法产生了一个加速。

Table 6. Comparison of CPU time for Example 3

表6. 例3的CPU时间比较

Method	$N = 72$ $M = 32$	$N = 144$ $M = 64$	$N = 288$ $M = 128$	$N = 576$ $M = 256$	$N = 1152$ $M = 512$
Present method	0.00566	0.00796	0.12430	0.32683	1.68447
Ref. [5]	0.03120	0.09360	0.32760	1.21681	4.83603

例4: 我们考虑以下二维时间延迟奇异摄动反应扩散问题

$$\begin{cases} \frac{\partial u}{\partial t} - \varepsilon_1 \frac{\partial^2 u}{\partial x^2} + (1+0.5xy) \frac{\partial u}{\partial x} + e^{x^2y} \frac{\partial u}{\partial y} + e^{x+y} (1+t)u - t(x+y)v - txr = 10t^2 \sin(x+y), \\ \frac{\partial v}{\partial t} - \varepsilon_2 \frac{\partial^2 v}{\partial x^2} + (5+x^2y) \frac{\partial v}{\partial x} + (3+\sin(x+y)) \frac{\partial v}{\partial y} - (x+y)u + (1+t)(3+x+y)v - t \sin(y)r = -5(1-e^{-t})(x^2+y^2), \\ \frac{\partial r}{\partial t} - \varepsilon_3 \frac{\partial^2 r}{\partial x^2} + (3-xy) \frac{\partial r}{\partial x} + (1+x+y) \frac{\partial r}{\partial y} - xy^2u - t(\sin x + \sin y)v + e^t(2+\cos(x+y))r = -4te^t \cos(xy), \end{cases}$$

具有初始边界条件

$$u(0, y, t) = 4y \sin(t), \quad v(0, y, t) = 0, \quad r(0, y, t) = 3(1-e^t),$$

$$u(x, 0, t) = 4x \sin(t), \quad v(x, 0, t) = 0, \quad r(x, 0, t) = 3(1-e^t),$$

$$u(x, y, 0) = v(x, y, 0) = r(x, y, 0) = 0,$$

$$u(1, y, t) = 4(1+y) \sin(t), \quad v(1, y, t) = yt^2, \quad r(1, y, t) = 3e^y(1-e^t),$$

$$u(x, 1, t) = 4(x+1) \sin(t), \quad v(x, 1, t) = xt^2, \quad r(x, 1, t) = 3e^x(1-e^t).$$

为了获得数值解, 我们运用相同的思想来分割具有更多元素的系统。

图5显示了当 $\varepsilon = 10^{-4}$ 时例3的数值解, 表7分别为第一, 第二, 第三分量 ε 值的结果。我们可以看到, ε 的值越小, 最大误差也越小。由此可见, 本文方法具有较好的精度。

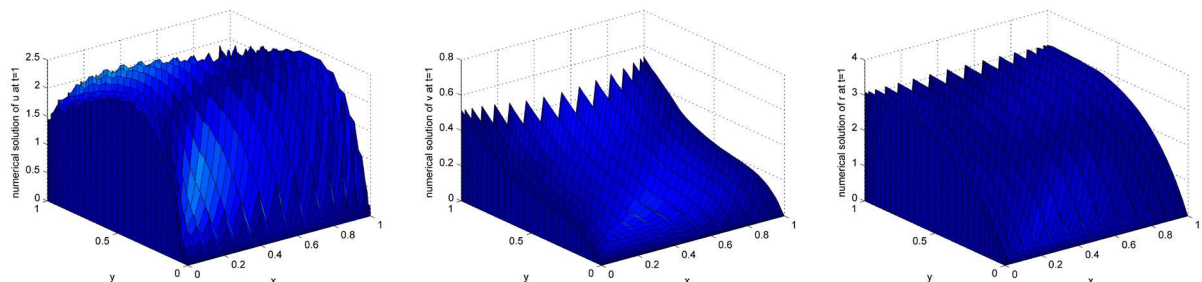


Figure 5. Numerical solution of Example 4 at $T=1$ for $\varepsilon=10^{-4}$ and $N=32, M=32$

图5. 在 $T=1$, $N=32, M=32$ 时例4的数值解

Table 7. Comparison of maximum errors and orders of convergence in Example 4 for v

表7. 例4中对 v 的最大误差和收敛阶数的比较

Ref. [11]	Present method							
	$N=16$ $M=8$	$N=32$ $M=16$	$N=64$ $M=32$	$N=128$ $M=64$	$N=16$ $M=8$	$N=32$ $M=16$	$N=64$ $M=32$	$N=128$ $M=64$
$\varepsilon_1 = 10^{-j}$	$6.6804E-2$	$5.7987E-2$	$3.9483E-2$	$2.4603E-2$	$7.8068E-4$	$5.6213E-4$	$4.27E-08$	$3.6216E-5$
	0.2042	0.5545	0.6824	0.7396	0.1083	0.4545	0.5532	0.6842
$\varepsilon_2 = 2^{-6}$	$6.8721E-2$	$5.8378E-2$	$4.0315E-2$	$2.5349E-2$	$7.9731E-4$	$5.7897E-4$	$8.3764E-5$	$3.8716E-5$
	0.2353	0.5341	0.6694	0.7285	0.1527	0.4721	0.5872	0.7011
$\varepsilon_3 = 2^{-8}$	$7.1566E-2$	$5.8489E-2$	$4.0574E-2$	$2.5602E-2$	$8.0124E-04$	$5.8849E-4$	$8.6019E-5$	$3.9663E-5$
	0.2911	0.5276	0.6643	0.7252	0.2352	0.4920	0.6013	0.7834
$\varepsilon_1 = 2^{-10}$	$7.2293E-2$	$5.8520E-2$	$4.0643E-2$	$2.5668E-2$	$8.2236E-4$	$5.9013E-4$	$8.3456E-5$	$4.0021E-5$
	0.3049	0.5259	0.6630	0.7242	0.2901	0.4971	0.6725	0.7991

4. 结论

在本文中，我们首次使用重心插值配点法来解决奇异摄动问题。该方法的一些计算结果与其他方法的比较表明，该方法具有较高的精度和收敛性。从这篇文章中，我们可以发现我们的方法可以应用于解决这样的人口统计模型。因此，我们可以将此方法扩展到更广泛的领域。本文的所有数值计算结果都是通过数学软件 MatlabR2007b 给出。

致 谢

感谢王玉兰老师的 support 与帮助。

参考文献

- [1] Shishkin, G.I. (1989) Approximation of Solutions of Singularly Perturbed Boundary Value Problems with a Parabolic Boundary Layer. *Computational Mathematics and Mathematical Physics*, **29**, 1-10. [https://doi.org/10.1016/0041-5553\(89\)90109-2](https://doi.org/10.1016/0041-5553(89)90109-2)
- [2] Shishkin, G.I. (1995) Mesh Approximation of Singularly Perturbed Boundary Value Problems for Systems of Elliptical and Parabolic Equations. *Computational Mathematics and Mathematical Physics*, **35**, 429-446.
- [3] Franklin, V., Paramasivam, M., et al. (2013) Second Order Parameter-Uniform Convergence for a Finite Difference Method for a Singularly Perturbed Linear Parabolic System. *International Journal of Numerical Analysis and Modeling.* **10**, 178-202.
- [4] Gracia, J.L., Lisbona, F.J. and O'Riordan, E. (2010) A Coupled System of Singularly Perturbed Parabolic Reaction-Diffusion Equations. *Advances in Computational Mathematics*, **32**, 43-61. <https://doi.org/10.1007/s10444-008-9086-3>
- [5] Kumar, M. and Rao, S.C.S. (2010) High Order Parameter-Robust Numerical Method for Time Dependent Singularly Perturbed Reaction-Diffusion Problems. *Computing*, **90**, 15-38. <https://doi.org/10.1007/s00607-010-0104-1>
- [6] Linss, T. and Madden, N. (2007) Parameter-Uniform Approximations for Time-Dependent Reaction-Diffusion Problems. *Numerical Methods for Partial Differential Equations*, **23**, 1290-1300. <https://doi.org/10.1002/num.20220>
- [7] MacMullen, H., Miller, J.J.H., O'Riordan, E. and Shishkin, G.I. (2001) A Second-Order Parameter-Uniform Overlapping Schwarz Method for Reaction-Diffusion Problems with Boundary Layers. *Journal of Computational and Applied Mathematics*, **130**, 231-244. [https://doi.org/10.1016/S0377-0427\(99\)00380-5](https://doi.org/10.1016/S0377-0427(99)00380-5)
- [8] Chandra Sekhara Rao, S. and Chawla, S. (2018) Numerical Solution of Singularly Perturbed Linear Parabolic System with Discontinuous Source Term. *Applied Numerical Mathematics*, **127**, 249-265. <https://doi.org/10.1016/j.apnum.2018.01.006>
- [9] Kumar, S. and Chandra Sekhara Rao, S. (2014) A Robust Overlapping Schwarz Domain Decomposition Algorithm for Time-Dependent Singularly Perturbed Reaction-Diffusion Problems. *Journal of Computational and Applied Mathematics*, **261**, 127-138. <https://doi.org/10.1016/j.cam.2013.10.053>
- [10] Clavero, C. and Jorge, J.C. (2019) An Efficient Numerical Method for Singularly Perturbed Time Dependent Parabolic 2D Convection—Diffusion Systems. *Journal of Computational and Applied Mathematics*, **354**, 431-444.
- [11] Schneiaer, C. and Werner, W. (1986) Some New Aspects of Rational Interpolation. *Mathematics of Computation*, **175**, 285-299. <https://doi.org/10.2307/2008095>
- [12] Berrut, J.P. (1984) Baryzentrische Formeln zur trigonometrischen Interpolation (I). *Zeitschrift fur angewandte Mathematik und Physik*, **35**, 91-105. <https://doi.org/10.1007/BF00945179>
- [13] Berrut, J.P. (1988) Rational Functions for Guaranteed and Experimentally Well Conditioned Global Interpolation. *Computers & Mathematics with Applications*, **15**, 1-16. [https://doi.org/10.1016/0898-1221\(88\)90067-3](https://doi.org/10.1016/0898-1221(88)90067-3)
- [14] Berrut, J.P. and Trefethen, L.N. (2004) Barycentric Lagrange Interpolation. *SIAM Review*, **46**, 501-517. <https://doi.org/10.1137/S0036144502417715>
- [15] Higham, N.J. (2004) The Numerical Stability of Barycentric Lagrange Interpolation. *IMA Journal of Numerical Analysis*, **24**, 547-556. <https://doi.org/10.1093/imanum/24.4.547>
- [16] Mascarenhas, W.F. (2014) The Stability of Barycentric Interpolation at the Chebyshev Points of the Second Kind. *Numerische Mathematik*, **128**, 265-300. <https://doi.org/10.1007/s00211-014-0612-6>
- [17] Li, S.P. and Wang, Z.Q. (2015) Barycentric Interpolation Collocation Method for Nonlinear Problems. National Defense Industry Press, Beijing.

- [18] Li, S.P. and Wang, Z.Q. (2012) High-Precision Non-Grid Center of Gravity Interpolation Collocation Method: Algorithm, Program and Engineering Application. Science Press, Beijing.
- [19] Wang, Y.L., Tian, D. and Li, Z.Y. (2017) Numerical Method for Singularly Perturbed Delay Parabolic Partial Differentiation Equations. *Thermal Science*, **21**, 1595-1599. <https://doi.org/10.2298/TSCI160615040W>
- [20] Liu, F.F., Wang, Y.L. and Li, S.G. (2018) Barycentric Interpolation Collocation Method for Solving the Coupled Viscous Burgers' Equations. *International Journal of Computer Mathematics*, **95**, 2162-2173. <https://doi.org/10.1080/00207160.2017.1384546>
- [21] Wu, H.C., Wang, Y.L. and Zhang, W. (2018) Numerical Solution of a Class of Nonlinear Partial Differential Equations by Using Barycentric Interpolation Collocation Method. *Mathematical Problems in Engineering*, **2018**, Article ID: 7260346. <https://doi.org/10.1155/2018/7260346>
- [22] Wu, H.C., Wang, Y.L., Zhang, W. and Wen, T. (2019) The Barycentric Interpolation Collocation Method for a Class of Nonlinear Vibration Systems. *Journal of Low Frequency Noise, Vibration and Active Control*, 1-10. <https://doi.org/10.1177/1461348418824898>
- [23] Zhou, X.F., Li, J.M., Wang, Y.L. and Zhang, W. (2019) Numerical Simulation of a Class of Hyperchaotic System Using Barycentric Lagrange Interpolation Collocation Method. *Complexity*, **2019**, Article ID: 1739785. <https://doi.org/10.1155/2019/1739785>
- [24] Li, J., Wang, Y.L. and Zhang, W. (2019) Numerical Simulation of the Lorenz-Type Chaotic System Using Barycentric Lagrange Interpolation Collocation Method. *Advances in Mathematical Physics*, **2019**, Article ID: 1030318. <https://doi.org/10.1155/2019/1030318>
- [25] Liu, H.Y., Huang, J., Pan, Y.B. and Zhang, J.P. (2018) Barycentric Interpolation Collocation Methods for Solving Linear and Nonlinear High-Dimensional Fredholm Integral Equations. *Computers Mathematics with Applications*, **327**, Article ID: 141154. <https://doi.org/10.1016/j.cam.2017.06.004>
- [26] Luo, W.H., Huang, T.Z., Gu, X.M. and Liu, Y. (2017) Barycentric Rational Collocation Methods for a Class of Nonlinear Parabolic Partial Differential Equations. *Applied Mathematics Letter*, **68**, 13-19. <https://doi.org/10.1016/j.aml.2016.12.011>

知网检索的两种方式：

1. 打开知网首页 <http://kns.cnki.net/kns/brief/result.aspx?dbPrefix=WWJD>
下拉列表框选择：[ISSN]，输入期刊 ISSN: 2324-7991，即可查询
2. 打开知网首页 <http://cnki.net/>
左侧“国际文献总库”进入，输入文章标题，即可查询

投稿请点击：<http://www.hanspub.org/Submission.aspx>
期刊邮箱：aam@hanspub.org